August 1982

New Perspectives on Electron Correlations

Anthony F. Starace
University of Nebraska-Lincoln, astarace1@unl.edu

Published in PHYSICS OF ELECTRONIC AND ATOMIC COLLISIONS, S. Datz, editor.

NEW PERSPECTIVES ON ELECTRON CORRELATIONS

Anthony F. Starace
Behlen Laboratory of Physics
The University of Nebraska
Lincoln, Nebraska 68588-0111
U.S.A.

Two formulations for describing electronic excitations developed by Fano and his school are reviewed. The transition matrix formulation of atomic photoionization has provided new perspectives on the well-known random phase approximation and on its relation to configuration interaction. The hyperspherical coordinate approach to two electron states and collision processes has provided new perspectives on the classification of two-electron excitation channels and on the evolution of highly excited electronic states.

I. INTRODUCTION

Ugo Fano and his school have made many contributions to atomic theory. A common feature of these many contributions is that they are "appropriate" formulations for particular physical problems. That is, they are formulations in which the key features of experimental observations stand out in an obvious way. Not surprisingly, given such an appropriate formulation, one is often provided with new perspectives. We shall concern ourselves here with some of the new perspectives that have been provided on electron correlations.

Specifically, we shall review in this paper two such appropriate formulations of Ugo Fano and his school which have in common that they treat effects of two electron excitations in particularly convenient ways. The first, the atomic transition matrix formulation for one-electron transition processes — in particular, for the single electron photoionization process — is designed to treat the effects of *virtual* pairs of excited electrons in addition to the usual final state interactions treated, for example, in a Hartree-Fock or close-coupling formulation. The atomic transition matrix formulation has provided new perspectives on the photoionization process and on the Random Phase Approximation (RPA) for describing this process. In particular, it has provided a new relation between the RPA and the more usual configuration interaction theory; and it has provided a more general definition of the RPA which permits one to treat open-shell atom photoionization processes in the same way as closed-shell atom photoionization processes.

The second appropriate formulation to be discussed here is the hyperspherical coordinate approach for describing the joint motion of two electrons and in particular *real* two electron excitation processes. This approach has shown that the radial and angular coordinates, in the six dimensional space appropriate for two electron systems, are approximately separable. This separability has in turn led to a new classification scheme for Rydberg series of two electron excitations. Most importantly, analysis of the breakdown of this approximate separability provides a new perspective on the evolution of two-electron excitations.

II. ATOMIC TRANSITION MATRIX FORMULATION

Theoretical understanding of closed-shell atom photoionization cross sections[1] has been based on the Random Phase Approximation (RPA),[2-4] which implies that, in addition to the usual final state interactions, virtual excitations of pairs of valence

electrons have an important influence on these cross sections. The importance of the electron correlations included in the RPA have been confirmed for closed-shell atoms by other theoretical methods, especially the Many-Body Perturbation Theory[5] and the R-Matrix Theory.[6] On the whole, RPA calculations — or their equivalent — agree with most experimental photoionization cross sections for closed-shell atoms to within about 10%.

The formal definition of the RPA is that, within a Hartree-Fock (HF) basis, one includes all particle-hole interactions to infinite order.[2] In particular, one must seemingly include an infinite number of virtually excited electron pair excitations and de-excitations. Given that the RPA works beautifully in describing atomic photoionization, the only additional wish that atomic physicists might have is for a closer relation between the RPA and the more familiar configuration interaction picture.

A. Closed-Shell Atom Treatment: Relation of the RPA to Configuration Interaction

With this in mind, Chang and Fano[7] developed the transition matrix formulation for closed-shell atom photoionization processes. Initial application was made to photoionization of the outer subshell of argon, i.e.,

$$Ar3p^6(^1S) + \gamma \rightarrow Ar^+3p^5(^2P)\varepsilon\ell(^1P) \ , \tag{1}$$

where dipole selection rules limit ℓ to the values 0 and 2. We shall use the process (1) to illustrate the theory. Chang and Fano[7] choose the following configurations for the initial and final states:

$$\langle f| \equiv \langle 3p^5 \, \psi_{\varepsilon d} \, (^1P)| \tag{2a}$$

$$|i\rangle \equiv |3p^6(^1S)\rangle + |3p^4\Phi_a\Phi_b \, (^1S)\rangle \tag{2b}$$

Thus the final state consists of a HF core of electrons plus an excited electron, with angular momentum 2 and kinetic energy ε, described by the unknown wavefunction $\psi_{\varepsilon d}(r)$. (Note that we ignore the s-channel in this discussion for simplicity; in any case, it is much weaker than the d-channel.) The initial state consists of a HF ground state $|3p^6(^1S)\rangle$ plus a correlation term having two electrons excited out of the HF ground state. These two electrons are described by the unknown wavefunctions $\Phi_a(r)$ and $\Phi_b(r)$, which we shall presume have orbital angular momentum 2.

The dipole matrix element between the initial and final states in Eq. (2) is:

$$\langle f|r^{(1)}|i\rangle = 2(\langle\psi_{\varepsilon d}|r|3p\rangle - \langle 3p|r|\phi\rangle) . \tag{3}$$

Here the matrix elements on the right represent radial integrals over r, the factor 2 is an overall angular factor, and the function $\phi(r)$ is defined as the following linear combination of the unknown correlation functions $\Phi_a(r)$ and $\Phi_b(r)$:

$$\phi(r) \equiv C(\Phi_a(r)\langle\psi_{\varepsilon d}|\Phi_b\rangle + \Phi_b(r)\langle\psi_{\varepsilon d}|\Phi_a\rangle) \tag{4}$$

In Eq. (4), C represents an angular factor and the brackets represent overlap integrals of Φ_a and Φ_b with $\psi_{\varepsilon d}$. It is because of these overlaps that Φ_a and Φ_b are assumed to have orbital angular momentum 2. Clearly, since the dipole operator is a one electron operator, the dipole transition matrix element between the correlation term in Eq. (2b) and the final state in Eq. (2a) is non-zero only if one of the virtually excited electrons, represented by the correlation function Φ_a or Φ_b, has a non-zero overlap with the excited electron function $\psi_{\varepsilon d}$. The other virtually excited electron, represented by Φ_b or Φ_a, is de-excited by the dipole interaction to the 3p-subshell.

To completely determine the dipole matrix element between the initial and final

states in Eq. (2) for a particular photon energy, then, one only needs to determine the unknown final state wavefunction $\psi_{\varepsilon d}(r)$ and the particular linear combination of the correlation functions $\Phi_a(r)$ and $\Phi_b(r)$ represented by $\phi(r)$ in Eq. (4). To determine $\psi_{\varepsilon d}(r)$ and $\phi(r)$, Chang and Fano[7] start from the equation of motion of the outer product $|f><i|$,

$$H|f><i| - |f><i|H = \hbar\omega\,|f><i| \quad , \tag{5}$$

where H is the exact Hamiltonian for the atom and $\hbar\omega$ is the photon energy. Eq. (5) is integrated analytically over N-1 radial coordinates to obtain a set of coupled differential equations in the Nth coordinate r for the unknown functions $\psi_{\varepsilon d}(r)$, $\Phi_a(r)$, and $\Phi_b(r)$. Upon performing these integrations, the first term on the left in Eq. (5) gives final state interactions, the second term on the left gives initial state interactions, and the right hand side gives the first order transition matrix,[7,8] from which the method gets its name. Chang and Fano then approximate the resulting equations by dropping all terms involving Φ_a and Φ_b which cannot be cast in terms of the linear combination $\phi(r)$ in Eq. (4). Further approximations are made, by dropping all but a few interactions involving $\phi(r)$, to obtain a coupled set of differential equations for $\psi_{\varepsilon d}(r)$ and $\phi(r)$ which can be shown[7] to be equivalent to the RPA.

The results of the transition matrix formulation for the photoionization of argon[9] are compared with experiment[10] in Fig. 1. Curves I show the length and velocity results obtained in the HF approximation which results from setting all interactions involving $\phi(r)$ equal to zero when calculating the final state wavefunction $\psi_{\varepsilon d}(r)$ in the transition matrix formulation. Curves II show the results obtained from solving the equations for $\psi_{\varepsilon d}$ and $\phi(r)$ in an uncoupled approximation. Finally, curves III show the results obtained by solving the coupled equations for $\psi_{\varepsilon d}(r)$ and $\phi(r)$. These latter results are in very good agreement with experiment[10] and are equivalent to results obtained in the RPA.[2] The difference between the transition matrix formulation and the RPA lies, however, in the closer relation of the former to a configuration interaction approach (cf. Eq. (2)). Indeed, the configuration interaction picture of Chang and Fano[7] has been confirmed directly by the multiconfiguration Hartree-Fock approach to photoionization of Swanson and Armstrong.[11]

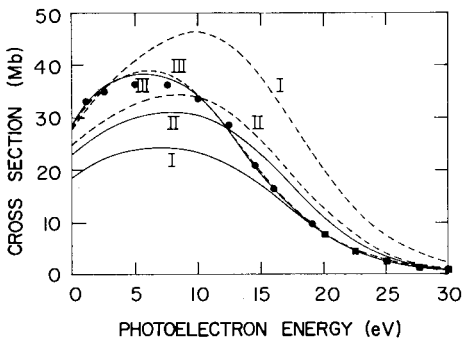

Fig. 1. Theoretical calculations of Chang[9] for the photoionization cross section of the 3p subshell of Ar. Dashed and solid lines give length and velocity results, respectively, in three levels of approximation discussed in the text. Experimentally measured values of the Ar cross section are indicated by the solid circles[10] and by the solid squares (Samson, unpublished) (from Ref. 9).

B. Open-Shell Atom Generalization: New Definition of the RPA

Theoretical understanding of the influence of electron correlations on the photoionization cross sections for open-shell atoms is less developed than for closed-

shell atoms. This is due to the greater theoretical difficulty of dealing with atoms which are not spherically symmetric and which thus have a greater number of final state channels. In addition, theoretical approximation methods developed specifically for closed-shell atoms, such as the RPA, are not easily generalized to treat open-shell atoms. In particular, while several open-shell atom RPA theories have been developed,[12-16] these have been given in the form of matrix or integral equations which require the use of large numbers of basis functions for their solution; furthermore, these RPA theories differ from one another.

Recently, Starace and Shahabi[17] generalized the transition matrix formulation to treat open- or closed-shell atoms. In order to do so, they developed a graphical procedure for evaluating the integrations over N-1 coordinates in each term of the equation of motion, Eq. (5). The graphical method simplifies the treatment of antisymmetry and of angular momentum algebra and at the same time affords an insight into the physical processes involved similar to that afforded by many-body perturbation theory graphs. The graphical method is based on the graphical angular momentum algebra of Jucys et al.[18] and on the state vector graphs of Briggs.[19]

Starace and Shahabi[17] start by defining the initial $\langle i|$ and final $|f^{\alpha}\rangle$ states in an open-shell atom photoionization process analogously to Chang and Fano's[7] states for closed-shell atoms, i.e.,

$$|f^{\alpha}\rangle \equiv \sum_{\tilde{L}\tilde{S}\ell} |n_o\ell_o^{q-1}(\tilde{L}\tilde{S})\psi^{\alpha}_{(\tilde{L}\tilde{S})\varepsilon\ell}\, L_f S_f\rangle \tag{6a}$$

$$\langle i| \equiv \langle n_o\ell_o^{q} L_i S_i| + \sum_{\substack{\overline{LS}\ell_\phi \\ L_pS_p}} b(\overline{LS}, L_pS_p, \ell_\phi)\langle n_o\ell_o^{q-2}(\overline{LS})\,\Phi_a\Phi_b\,(L_pS_p)L_iS_i| \,. \tag{6b}$$

Thus, the initial state is represented not only by the HF state of q electrons in the $n_o\ell_o$ subshell but also by correlation terms having two electrons excited out of the $n_o\ell_o$ subshell.

Using Eq. (6) for the form of the initial and final states, the graphical method permits the exact evaluation of all matrix elements in the equation of motion, Eq. (5), integrated over N-1 radial coordinates. Of these matrix elements, those involving the correlated part of the initial state are very complex. Starace and Shahabi[17] found, however, that if all interactions of the correlation functions Φ_a and Φ_b with the ionic core, $n_o\ell_o^{q-2}$, are approximated by requiring Φ_a and Φ_b to exchange zero orbital and spin angular mometum with the ionic core, then each interaction may be described in terms of linear combinations ϕ of Φ_a and Φ_b, as in the closed-shell atom case. Furthermore when the weight factors for these particular interactions are calculated as if the ionic core contained a full subshell of electrons, instead of only q-2 electrons, then in the closed-shell atom case the resulting coupled differential equations are identical to those obtained algebraically by Chang and Fano, which are equivalent[7] to the RPA equations.

The approximation that the virtually excited electrons Φ_a and Φ_b exchange zero angular momentum with the ionic core provides then a set of equations equivalent to the RPA equations in the closed-shell atom case. It thus provides also a new definition of the RPA. Since this new definition is independent of whether the atom is initially open or closed, it therefore provides a new RPA-equivalent set

of equations for open-shell atoms as well as a new understanding of the RPA.

In summary form, then, the key RPA-type approximations of the generalized transition matrix formulation for atomic photoionization are as follows:

(a) The ground state $\langle i|$ should include configurations of the form $\langle n_o \ell_o^{q-2} \Phi_a \Phi_b|$, in which two electrons are excited.

(b) When Φ_a or Φ_b interact with the core $n_o \ell_o^{q-2}$, one only includes the part of the interaction in which there is zero exchange of orbital and spin angular momenta.

(c) The approximate interactions in (b) are calculated with a weight factor appropriate for a filled $n_o \ell_o$ subshell.

These approximations give exactly the Chang-Fano equations[7] for closed-shell atoms and they give the close-coupling equations[20] when the correlation functions Φ_a and Φ_b are set equal to zero. The close connection to configuration interaction and the clear specification of the kinds of interactions included give a very good understanding of the RPA and its physical content.

III. HYPERSPHERICAL COORDINATE APPROACH

While the use of hyperspherical coordinates to describe two-electron correlations is quite old,[21-28] it is only relatively recently that Macek[29] introduced a quasi-separable approximation in such coordinates which provided quantitatively accurate predictions of doubly-excited-state energies in He as well as a good description of two-electron dynamics. The initial success of the quasi-separable approximation stimulated Fano and his school to further develop the theory and to carry out numerous applications to doubly excited states[30-36] of He and H^- as well as to continuum processes[37-39] for He and for the e-H system. Most recently the hyperspherical coordinate approach has been extended successfully to treat atoms with more than two electrons.[40-44] While the quasi-separable approximation is only the zero order approximation to a general theory of atomic collisions,[45] it has provided new perspectives which we review here on electron correlations and on the electron excitation process.

A two electron wavefunction $\psi(\vec{r}_1, \vec{r}_2)$ is usually described by the six coordinates r_1, r_2, $\hat{r}_1$, and $\hat{r}_2$ of the two electrons. In hyperspherical coordinates the magnitudes of the individual coordinates, r_1 and r_2, are replaced by the hyperspherical radius $R \equiv (r_1^2 + r_2^2)^{1/2}$ and the hyperspherical angle $\alpha \equiv \arctan(r_2/r_1)$. Before summarizing the features of the Schrödinger equation in these coordinates let us look first at plots of approximate two-electron probabilities, $|\psi(R,\alpha,\hat{r}_1,\hat{r}_2)|^2$, in these coordinates. Fig. 2 shows contour plots[31,32] and Fig. 3 shows relief maps[36] for the probability distributions of the singly-excited state $1s2s\ ^1S$ and the doubly-excited state $2s^2\ ^1S$ of He. (Note that the wavefunctions are calculated in the approximation that each electron has an orbital angular momentum equal to zero in order to eliminate all dependence on the angular variables $\hat{r}_1$ and $\hat{r}_2$; since the angular dependence is trivial, these states are symmetric about $\alpha = \pi/4$, i.e., under interchange of r_1 and r_2.)

The most obvious distinguishing features of the two probability distributions is that that for the single excited state is largest along $\alpha \simeq 0$ and $\alpha \simeq \pi/2$ (implying one electron is much further from the nucleus than the other) while that for the doubly excited state is largest along $\alpha \simeq \pi/4$ (implying both electrons

are comparably excited, i.e., $\alpha = \pi/4$ when $r_1 = r_2$). A second important feature is the behavior of the nodal lines for the two probability distributions. The $1s2s\ ^1S$ state has a single nodal line along $R \simeq 2$, while the $2s^2\ ^1S$ state has two nodal lines along $\alpha \simeq$ constant: one along $5° \lesssim \alpha \lesssim 30°$ and the other along $60° \lesssim \alpha \lesssim 85°$. The fact that the pattern of nodal lines is approximately along the orthonormal grid of constant R and constant α implies a quasi-separability of R and α coordinates.

The nodal line pattern for a particular state serves also to classify the state.[36] The ground state of He, $1s^2\ ^1S$, has a spherically symmetric probability distribution and is the first member of the singly-excited state channel $1sns\ ^1S$ which converges to the $He^+(n=1)$ threshold. The single node in R for the state $1s2s\ ^1S$, shown in Figs. 2(a) and 3(a), characterizes it as the second member of the $1sns\ ^1S$ channel. The state $2s^2\ ^1S$, shown in Figs. 2(b) and 3(b), has no radial nodes. It is the first member of the Rydberg series $2sns\ ^1S$ converging to

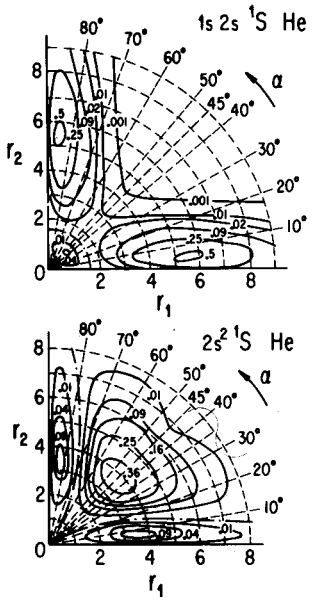

Fig. 2. Contour plot of the approximate probability distribution $|\psi(\vec{r}_1,\vec{r}_2)|^2$ for He. (a) $1s2s\ ^1S$ (b) $2s^2\ ^1S$. Solid Lines: lines of constant probability. Dot-Dash Lines: nodal lines. (From Ref. 32)

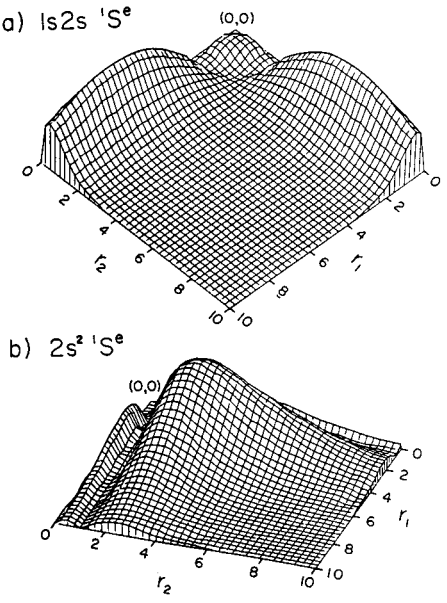

Fig. 3. Relief map of the approximate probability distribution $|\psi(\vec{r}_1,\vec{r}_2)|^2$ for He. (a) $1s2s\ ^1S$ (b) $2s^2\ ^1S$ (From Ref. 36)

the $He^+(n=2)$ threshold. The two nodes approximately along constant α, symmetrical about $\alpha = \pi/4$, characterize $2s^2\ ^1S$ as a member of this second Rydberg channel. Thus nodes in R characterize the excitation of a state within a channel while nodes in α characterize the various channels.[36]

These features of the two-electron wavefunction $\psi(\vec{r}_1,\vec{r}_2)$, in the hyperspherical coordinates R and α, motivate the hyperspherical method of Macek,[29] who expands $\psi(\vec{r}_1,\vec{r}_2)$ in terms of a complete set of adiabatic angle functions $\phi_\mu(R;\alpha,\hat{r}_1,\hat{r}_2)$:

$$\psi_E(R,\alpha,\hat{r}_1,\hat{r}_2) = (R^{5/2}\sin\alpha\cos\alpha)^{-1} \sum_\mu F_{\mu E}(R)\phi_\mu(R;\alpha,\hat{r}_1,\hat{r}_2) \tag{7}$$

The angle functions $\phi_\mu(R;\alpha,\hat{r}_1,\hat{r}_2)$ are dependent on the five angles α, $\hat{r}_1$, and $\hat{r}_2$ and are only parametrically dependent on R. They are the eigenstates of the following differential equation,

$$\left[\frac{-d^2}{d\alpha^2} + \frac{\vec{\ell}_1^{\,2}}{\sin^2\alpha} + \frac{\vec{\ell}_2^{\,2}}{\cos^2\alpha} - RC(\alpha,\theta_{12})\right]\phi_\mu = -U_\mu(R)\phi_\mu \quad , \tag{8}$$

and the potentials $U_\mu(R)$ are the corresponding eigenvalues at each value of R. In Eq. (8), the potential $-C(\alpha,\theta_{12})$ is proportional to the sum of the nuclear and electrostatic potentials,

$$-C(\alpha,\theta_{12}) = -\frac{Ze^2}{\cos\alpha} - \frac{Ze^2}{\sin\alpha} + \frac{e^2}{(1-\sin 2\alpha\cos\theta_{12})^{1/2}} \tag{9}$$

Substituting Eq. (7) into the two-electron Schrödinger equation and using the properties of the angle functions ϕ_μ in Eq. (8), one obtains the following set of coupled differential equations for the radial functions $F_{\mu E}(R)$:

$$\left(\frac{d^2}{dR^2} + \frac{U_\mu(R)+\frac{1}{4}}{R^2} + 2E\right)F_{\mu E}(R) + \sum_{\mu'} W_{\mu,\mu'}\,F_{\mu' E}(R) = 0 \quad , \tag{10}$$

where

$$W_{\mu,\mu'} \equiv \left(\phi_\mu, \frac{\partial^2\phi_{\mu'}}{\partial R^2}\right) + 2\left(\phi_\mu, \frac{\partial\phi_{\mu'}}{\partial R}\right)\frac{\partial}{\partial R} \quad . \tag{11}$$

The brackets in Eq. (11) imply integration over angular variables only.

Each of the potentials $U_\mu(R)$ and its corresponding angular eigenfunction ϕ_μ define the set of hyperspherical, two-electron channels μ. These channels are coupled through the radial derivative matrix elements $W_{\mu,\mu'}$ in Eq. (11). In the separable — or adiabatic — approximation[29] one assumes that motion in α and motion in R are weakly coupled so that the derivatives of ϕ_μ in Eq. (11) are small enough that one may ignore the coupling terms $W_{\mu,\mu'}$. In this case, the two electron wavefunction may be represented by a single term in the summation in Eq. (7):

$$\psi^{sep.}_{\mu E}(R,\alpha,\hat{r}_1,\hat{r}_2) = (R^{5/2}\sin\alpha\cos\alpha)^{-1} F_{\mu E}(R)\phi_\mu(R;\alpha,\hat{r}_1,\hat{r}_2) \quad (12)$$

Notice in Eq. (12) how all members of the channel μ have the same angular function ϕ_μ. Each state of excitation energy E within the channel μ is described by the radial function $F_{\mu E}$, which is calculated in the channel potential $U_\mu(R)$ using Eq. (10) and ignoring the coupling terms. Because each member of a Rydberg series of doubly excited states has the same angular function ϕ_μ and has a radial function $F_{\mu E}(R)$ that is calculated in the same potential $U_\mu(R)$, the physical properties of states belonging to a particular channel μ are often immediately apparent upon examination of $U_\mu(R)$ and ϕ_μ. In what follows we illustrate the use of the potentials $U_\mu(R)$ to classify two-electron excitation channels. We then examine the numerical accuracy of the separable approximation. Next, we show how the variation of the angle functions ϕ_μ with R provides a new perspective on the evolution of excitation processes. Lastly, we sketch very recent extensions of the hyperspherical coordinate approach to atoms having more than two electrons.

A. Hyperspherical Classification of Two-Electron Excitation Channels

The first major success[29] of the separable approximation in hyperspherical coordinates was the classification and interpretation of the photoabsorption spectrum of He in the region of the doubly excited Rydberg states converging to the n = 2 threshold. In the usual classification scheme there should be three Rydberg series of such levels of comparable intensity: 2snp ^{1}P, 2pnd ^{1}P, and 2pns ^{1}P. The experimental spectrum of Madden and Codling,[46] shown in Fig. 4, showed only one strong Rydberg series and one very weak Rydberg series. The third possible series was not observed. Cooper, Fano, and Prats[47] interpreted the relative intensities of the two observed series in terms of the so-called "+" and "-" series, $(2snp \pm 2pns)\,^1$P. The "+" series members are more intense than those of the "-" series because the corresponding wavefunctions of the "+" members have a much larger amplitude near the origin, allowing therefore a much larger overlap with the ground state. This scheme, however, does not explain the weakness of the 2pnd ^{1}P channel. Fig. 5, however, shows Macek's hyperspherical potentials $U_\mu(R)$ for the three channels μ converging to the n=2 state of He^+. One sees immediately that the three channels have vastly different centrifugal barriers near the origin, explaining the large intensity differences of the three allowed channels. Furthermore, the first two hyperspherical channels have the "+" and "-" characteristics predicted by Cooper et al.[47]

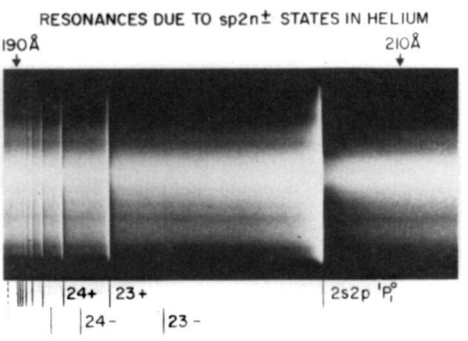

Fig. 4. Photoabsorption spectrum of He between 190 and 210 Å. The "+" and "-" series members are indicated below the spectrum. (From Ref. 46)

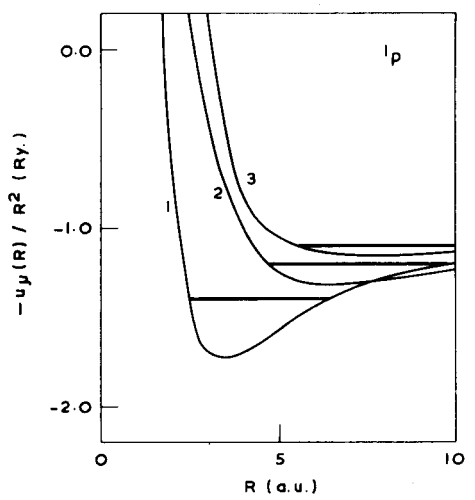

Fig. 5. Hyperspherical potential curves U_μ/R^2 vs R for the three He doubly excited ^1P channels converging to the n=2 state of He^+. (From Ref. 29).

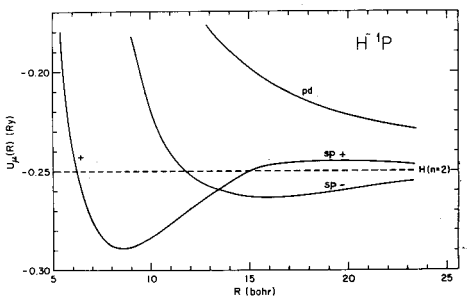

Fig. 6. Hyperspherical potential curves U_μ vs R for the three H^- doubly excited ^1P channels converging to the n=2 state of H. (From Ref. 33)

Similar work has been carried out for the doubly excited states of H^- by Lin[33] and by Greene.[35] Fig. 6 shows Lin's[33] hyperspherical potentials for the three doubly excited Rydberg series converging to the n=2 state of H. The "+" channel is repulsive at large R and is not deep enough to support any bound states at small R. The repulsive barrier can, however, produce shape resonances in this channel above threshold. The "-" potential is attractive at large R and can support an infinity of Feshbach resonances. The "pd" channel is repulsive at all R values. Fig. 7 shows Greene's hyperspherical potentials for doubly excited channels converging to the n=3 state of H. In this case the "+" potential is always attractive and since its centrifugal barrier is weaker than those of the other channels, the "+" series is the most strongly excited from the ground state. Greene used this hyperspherical channel calculation and quantum defect theory (QDT) to interpret the resonances obtained by Hamm et al.[48] in the photodetachment spectrum of H^- near the n=3 threshold as due to the "+" series resonances. The data and Greene's QDT fit are in excellent agreement, as shown in Fig. 8.

B. Numerical Results in the Separable Approximation

The separable approximation in hyperspherical coordinates thus provides a very accurate qualitative description of Rydberg series of doubly excited states in He and H^-. But how good are the quantitative predictions in this approximation? The answer depends on the excitation energy above the minimum in the hyperspherical potential U_μ of interest. For the lowest energy members calculated in the potentials $U_\mu(R)$, the separable approximation energies are in excellent agreement with experiment and with other theoretical results; the separable approximation wavefunction may also be used confidently. However, higher energy members of a particular channel μ calculated in the potential $U_\mu(R)$ are increasingly too high in energy,[29] if bound, or have too negative phase shifts,[37-39] if unbound. This is not surprising since for higher excitation energies the coupling between the hyperspherical channels can no longer be ignored. Thus at present the separable approximation in the hyperspherical coordinate

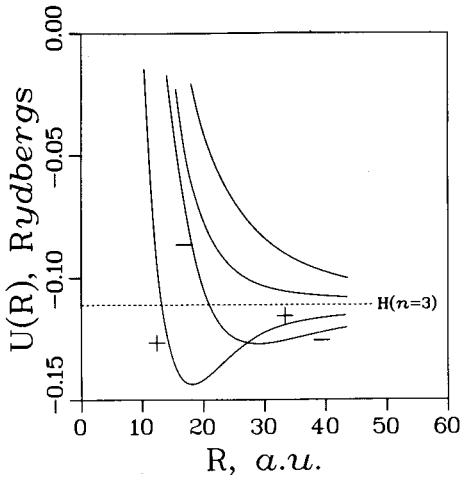

Fig. 7. Hyperspherical potential curves U_μ vs R for H^- doubly excited ^1P channels converging to the n=3 threshold of H. (From Ref. 35)

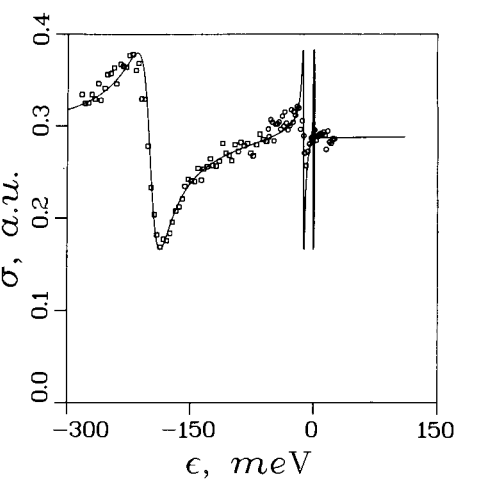

Fig. 8. Photodetachment cross section of H^- near the n=3 threshold of H at $\varepsilon = 0$. Data: Hamm et al.[48] Solid Line: QDT fit of Greene.[35] (From Ref. 35)

approach provides a very good initial approximation to the exact electron wavefunction, but its systematic improvement for states of moderate and high excitation energy to provide state-of-the-art numerical predictions has only just begun[38,41] and remains a task for future research.

In what follows, we provide a few examples of the high level of accuracy to be expected from the separable approximation for the lowest excited states in particular hyperspherical potentials. Regarding level energies, Macek[29] calculated the He $2s2p(^1P)$ resonance excitation energy as 68.138 eV as compared with the experimental value[46] of 60.135 ± .015 eV. Similarly, Miller and Starace[39] calculated the ground state energy of He as -2.895 a.u. as compared with the essentially exact non-relativistic theoretical value[49] of -2.904 a.u. Regarding phase shifts, Lin[37] calculated the e-H ^1S phase shift at k = 0.1 to be 2.513 rad. as compared with the essentially exact theoretical value[50] of 2.553 rad.

Lastly, a recent calculation[39] of the photoionization cross section of He using separable approximation hyperspherical coordinate wavefunctions demonstrates the strengths and weaknesses of the method. The initial and final wavefunctions for the process

$$He(^1S) + \gamma \longrightarrow He^+ 1s(^2S) + e^-(^1P) \qquad (13)$$

both have the form of Eq. (12). For the initial state, μ corresponds to the lowest ^1S potential $U_\mu(R)$, and for the final state, μ corresponds to the lowest ^1P potential $U_\mu(R)$. The photoionization cross section obtained using the separable approximation wavefunctions is shown in Fig. 9.

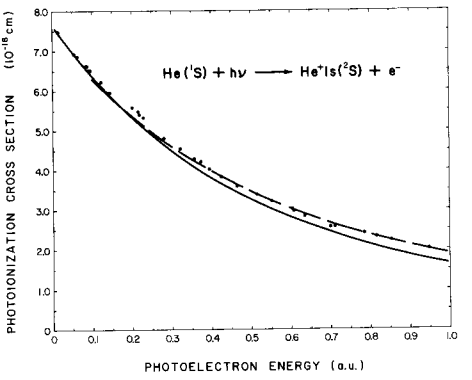

Fig. 9. Photoionization cross section for He. Full curve: separable approximation (single channel) hyperspherical calculation of Miller and Starace (Ref. 39); Dots: Experimental results of Samson (Ref. 51); Dashed Curve: 1s-2s-2p (four channel) close-coupling calculation of Jacobs (Ref. 52) (From Ref. 39).

Fig. 9 also shows the revised experimental results of Samson,[51] which have error bars of ±3%. The results lie within these error limits near threshold (for kinetic energies $0.0 \leq \varepsilon \leq 0.4$ a.u.) and in fact agree with experiment to within 1% at threshold. The hyperspherical results, however, are systematically lower than experiment above $\varepsilon = 0.4$ a.u. Of the many other theoretical calculations, we show the one with the best overall agreement with experiment: the four channel (1s-2s-2p) close-coupling calculation of Jacobs.[52] In comparison with the close-coupling results, the hyperspherical results are in better agreement with experiment below $\varepsilon = 0.2$ a.u. and are systematically lower above $\varepsilon = 0.2$ a.u.

C. Evolution of Two-Electron Excitations

The hyperspherical coordinate approach has not only been used to study stationary states, but also to understand qualitatively how a low-energy two electron state concentrated near the origin, upon receiving energy during a collision process, evolves to states of high excitation far from the origin. The key idea, stressed recently by Fano[53] and illustrated graphically by Lin,[36] is that such states describe motion along a potential ridge centered about the direction $\alpha = \pi/4$ (i.e., $r_1 = r_2$).

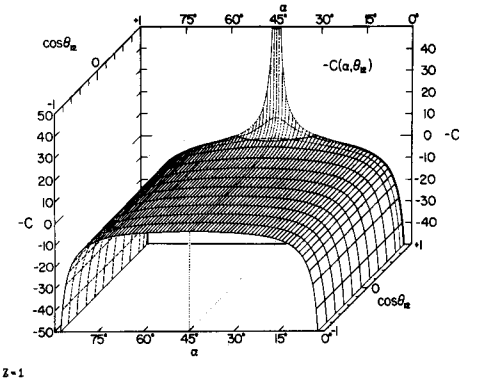

Fig. 10. Relief map of the potential $-C(\alpha,\theta_{12})$ defined in Eq. (9) for Z = 1. (from Ref. 32).

Consider Eq. (8) for the channel functions $\phi_\mu(R;\alpha,\hat{r}_1,\hat{r}_2)$. The potential $-C(\alpha,\theta_{12})$, defined in Eq. (9), is shown in Fig. 10 for Z = 1. States having one electron more excited than the other, i.e., $r_2 \gg r_1$ or $r_1 \gg r_2$, have an angle function ϕ_μ with maximum amplitude in the valleys of the potential in Fig. 10, near $\alpha = 0$ and $\alpha = \pi/2$. Comparably excited, doubly-excited states have $r_1 \sim r_2$ and thus the angle function ϕ_μ for these states has maximum amplitude on the ridge of the potential in Fig. 10, near $\alpha = \pi/4$, and preferably near $\cos\theta_{12} = -1$ (i.e., on opposite sides of the nucleus). We consider

now the R-dependence of the angle functions ϕ_μ. Eq. (8) shows that the potential -C is multiplied by R. For large enough R, therefore, the potential -RC on the ridge becomes equal to the eigenvalue $U_\mu(R)$. At this "classical turning point" the angle function ϕ_μ has no more "kinetic energy" of motion in α on the ridge. For larger R values, its amplitude on the ridge is exponentially damped and the probability amplitude in the channel μ must retreat to the valleys of the potential in Fig. 10, implying that for such large R values μ describes states with one electron more highly excited than the other. Alternatively, the two electron state on the ridge may "hop" to the next higher channel μ'. With a higher value of $-U_{\mu'}(R)$, the two electron excitation could move to somewhat larger R along the ridge since the difference between $-U_{\mu'}$ and the top of the potential ridge of -RC would restore some positive "kinetic energy" of motion in α. Actually the vicinity of the classical turning point is propitious for such a transition to a higher channel μ' since the coupling matrix elements (cf. Eq. (11)) are largest precisely where the channel functions are changing most rapidly with R.

Lin[36] has shown graphically how the channel functions ϕ_μ behave as functions of R.

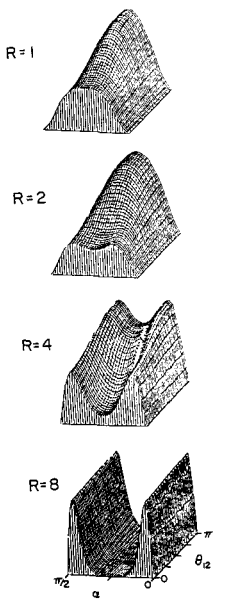

Fig. 11. Plot of $|\phi_\mu(R;\alpha,\theta_{12})|^2$ vs. α and θ_{12} for various R values for the first H^- ^1S hyperspherical channel $\mu = 1$. (from Ref. 36)

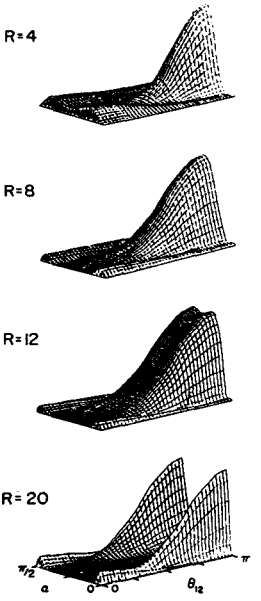

Fig. 12. Plot of $|\phi_\mu(R;\alpha,\theta_{12})|^2$ vs. α and θ_{12} for various R values for the second H^- ^1S hyperspherical channel $\mu = 2$. (from Ref. 36)

In Figs. 11 and 12 we show the $H^-(^1S)$ channel functions $\phi_\mu(R;\alpha,\theta_{12})$ for $\mu = 1$ and $\mu = 2$ (i.e., the lowest two ^1S hyperspherical channels). In Fig. 11 one sees that at $R = 1$ the charge distribution in the first channel is peaked about $\alpha = \pi/4$, lying on the potential ridge. At $R = 4$, however, the charge distribution is vacating the ridge and moving to the valleys near $\alpha = 0$ and $\alpha = \pi/2$. By $R = 8$, $\mu = 1$ describes a channel with one electron much more highly excited than the other. Fig. 12 shows the next higher hyperspherical channel function. Note that at $R = 4$, precisely where $\mu = 1$ has a depression along the ridge, the $\mu = 2$ channel's charge distribution has a maximum. This peak in $\mu = 2$ along the ridge progresses outward to larger R values until at $R = 12$ a depression appears along the ridge. If two-electron states in $\mu = 2$ are to move to larger R and remain comparably excited they must hop again to the next higher hyperspherical channel, and so on.

This new perspective of two electron excitation states evolving toward large radii R along a potential ridge has its origins in the Wannier-Peterkop-Rau[54] analysis of electron impact ionization near threshold. Its application to quantitative predictions of excitation cross sections remains a task for future research.

D. Recent Extensions to Atoms Having More than Two Electrons

The new perspectives on electron correlations provided by the hyperspherical coordinate approach are not limited to He and H^-. Indeed several applications have already been made to heavier atoms. While detailed discussion of these works is not possible in this short paper, we wish to alert the reader to this recent progress. Firstly, Clark and Greene[40] have made a first attempt at a hyperspherical description of the three electron systems Li and H^{--}. Greene,[41] on the other hand, has treated Be and the alkaline earth atoms as two electron systems, outside closed shells, in hyperspherical coordinates. The influence of the inner closed shells on the outer electron pair is approximated by an atomic potential. Watanabe[42] has gone still further in treating two electrons in hyperspherical coordinates outside an open-shell ionic core. The influence of the ionic core on the outer electrons is described by appropriate boundary conditions on the hyperspherical wavefunction at the surface of the ionic core. Both K^- and He^- have been treated in this way. Lastly, Lin[44] has presented a method for generating basis sets of analytically determined, approximate hyperspherical wavefunctions. Such basis sets might be used to describe doubly excited states of complex atoms in perturbation or scattering calculations.

ACKNOWLEDGMENTS

The author wishes to thank U. Fano, C. D. Lin, C. H. Greene, and S. Watanabe for providing results prior to publication. Research support of the National Science Foundation under Grant No. PHY-8026055 is also gratefully acknowledged.

REFERENCES

1. Starace, A. F., "Trends in the Theory of Atomic Photoionization," Applied Optics 19, 4051 (1980); "Theory of Atomic Photoionization," in Handbuch der Physik 31, Mehlhorn, W. (ed.) (Springer-Verlag, Berlin, 1982).

2. Amusia, M. Ya and Cheripkov, N. A., Case Studies in Atomic Physics 5, 47 (1975).

3. Wendin, G., in: Wuilleumier, F. J. (ed.) Photoionization and Other Probes of Many-Electron Interactions (Plenum Press, New York, 1976), p. 61.

4. Johnson, W. R. and Lin, C. D., Phys. Rev. A 20, 964 (1979); Johnson, W. R. and Cheng, K. T., Phys. Rev. A 20, 978 (1979); Huang, K.-N., Johnson, W. R., and Cheng, K. T., Phys. Rev. Lett. 43, 1658 (1979).

5. Kelly, H. P., in: Wuilleumier, F. J. (ed.), Photoionization and Other Probes of Many-Electron Interactions (Plenum Press, New York, 1976), p. 83.

6. Burke, P. G. and Robb, W. D., Adv. Atomic Mol. Phys. 11, 143 (1975); Burke, P. G. and Taylor, K. T., J. Phys. B 8, 2620 (1975).

7. Chang, T. N. and Fano, U., Phys. Rev. A 13, 263 (1976); Phys. Rev. A 13, 282 (1976).

8. Löwdin, P. O., Phys. Rev. 97, 1474 (1955).

9. Chang, T. N., Phys. Rev. 15, 2392 (1977).

10. Samson, J. A. R., Adv. At. Mol. Phys. 2, 177 (1966).

11. Swanson, J. R. and Armstrong, Jr., L., Phys. Rev. A 15, 661 (1977); Phys. Rev. A 16, 1117 (1977).

12. Armstrong, Jr., L., J. Phys. B 7, 2320 (1974).

13. Rowe, D. J. and Ngo-Trong, C., Rev. Mod. Phys. 47, 471 (1975).

14. Dalgaard, E., J. Phys. B 8, 695 (1975).

15. Starace, A. F. and Armstrong, Jr., L., Phys. Rev. A 13, 1850 (1976).

16. Cherepkov, N. A. and Chernysheva, L. V., Phys. Letters 60A, 103 (1977); Izvestia Akademii Nauk SSSR 41, 2518 (1977) [Eng. Translation: Akademiia Nauk SSSR. Bulletin Physical Series (Allerton Press) 41, 47 (1977).]

17. Starace, A. F. and Shahabi, S., Physica Scripta 21, 368 (1980); Phys. Rev. A (in press).

18. Yutsis (Jucys), A. P., Levinson, I. B., and Vanagas, V. V., The Theory of Angular Momentum (Israel Program for Scientific Translations, Jerusalem, 1962).

19.

19. Briggs, J. S., Rev. Mod. Phys. 43, 189 (1971).

20. Smith, K., Henry, R. J. W., and Burke, P. G., Phys. Rev. 147, 21 (1966).

21. Kemble, E. C., The Fundamental Principles of Quantum Mechanics with Elementary Applications, (Dover Publications, Inc. New York 1937) p. 210.

22. Morse, P. M. and Feshbach, H., Methods of Theoretical Physics, Vol. II (McGraw-Hill Book Company, New York, 1953) pp. 1730ff.

23. Fock, V., Izvest. Acad. Nauk USSR ser Fiz. 18, 161 (1954) [Eng. Transl.: Kong. Norske Videnskabers Selskabs Forh. 31, 138, 145 (1958).]

24. Demkov, Y. N. and Ermolaev, A. M., Zh. Eksp. Teor. Fiz. 36, 896 (1959) [Sov. Phys. - JETP 36, 633 (1959)].

25. Smith, F. T., Phys. Rev. 120, 1058 (1960).

26. Zickendraht, W., Annals of Physics 35, 18 (1965).

27. Frankowski, K. and Pekeris, C. L., Phys. Rev. 146, 46 (1966); Frankowski, K., Phys. Rev. 160, 1 (1967).

28. Macek, J. H., Phys. Rev. 160, 170 (1967).

29. Macek, J. H., J. Phys. B 2, 831 (1968).

30. Fano, U., Atomic Physics 1 (Plenum, New York, 1969), pp. 209-25.

31. Fano, U. and Lin, C. D. Atomic Physics 4 (Plenum, New York, 1975), pp. 47-70.

32. Lin, C. D., Phys. Rev. A 10, 1986 (1974).

33. Lin, C. D., Phys. Rev. Lett. 35, 1150 (1975); Phys. Rev. A 14, 30 (1976).

34. Klar, H., J. Phys. B. 7, L436 (1974); Klar, H. and Klar, M., J. Phys. B 13, 1057 (1980).

35. Greene, C. H., J. Phys. B 13, L39 (1980).

36. Lin, C. D., Phys. Rev. A (in press).

37. Lin, C. D., Phys. Rev. A 12, 493 (1975).

38. Klar, H. and Fano, U., Phys. Rev. Lett. 37, 1132 (1976); Klar, H., Phys. Rev. A 15, 1452; Klar, H. and Klar, M., Phys. Rev. A 17, 1007 (1978).

39. Miller, D. L. and Starace, A. F., J. Phys. B 13, L525 (1980).

40. Clark, C. W. and Greene, C. H., Phys. Rev. A 21, 1786 (1980).

41. Greene, C. H., Phys. Rev. A 23, 661 (1981).

42. Watanabe, S., Phys. Rev. A (in press).

43. Fano, U., Physica Scripta (in press).

44. Lin, C. D., Phys. Rev. A 23, 1585 (1981).

45. Fano, U., Phys. Rev. A (in press).

46. Madden, R. P. and Codling, K., Astrophys. J. 141, 364 (1965).

47. Cooper, J. W., Fano, U., and Prats, F., Phys. Rev. Lett. 10, 518 (1963).

48. Hamm, M. E., Hamm, R. W., Donahue, J., Gram, P. A. M., Pratt, J. C., Yates, M. A., Bolton, R. D., Clark, D. A., Bryant, H. C., Frost, C. A., and Smith, W. W., Phys. Rev. Lett. 43, 1715 (1979).

49. Pekeris, C. L., Phys. Rev. 112, 1649 (1958).

50. Schwartz, C., Phys. Rev. 124, 1468 (1961).

51. Samson, J. A. R., Phys. Reports 28C, 303 (1976).

52. Jacobs, V. L., Phys. Rev. A 3, 289.(1971).

53. Fano, U., Phys. Rev. A 22, 2660 (1980).

54. Wannier, G., Phys. Rev. 90, 817 (1953); Peterkop, R., J. Phys. B 4, 513 (1971); Rau, A. R. P., Phys. Rev. A 4, 207 (1971).